

Inventories and concentration profiles of ^{137}Cs in undisturbed soils in the northeast of Buenos Aires Province, Argentina

M.L. Montes, L.M.S. Silva, C.S.A. Sá, J. Runco, M.A. Taylor, J. Desimoni

ABSTRACT

Inventories and vertical distribution of ^{137}Cs were determined in La Plata region undisturbed soils, Argentina. A mean inventory value of $891 \pm 220 \text{ Bq/m}^2$ was established, which is compatible with the values expected from atmospheric weapon tests fallout. The study was complemented with pH, organic carbon fraction, texture and mineralogical soil analyses. Putting together Southern Hemisphere ^{137}Cs inventory data, it is possible to correlate these data with the mean annual precipitations. The large differences in ^{137}Cs concentration profiles were attributed to soil properties, especially the clay content and the pH values.

A convection–dispersion model with irreversible retention was used to fit the activity concentration profiles. The obtained effective diffusion coefficient and effective convection velocity parameters values were in the range from $0.2 \text{ cm}^2/\text{y}$ to $0.4 \text{ cm}^2/\text{y}$ and from $0.23 \text{ cm}/\text{y}$ to $0.43 \text{ cm}/\text{y}$, respectively. These data are in agreement with values reported in literature. In general, with the growth of clay content in the soil, there was an increase in the transfer rate from free to bound state. Finally, the highest transfer rate from free to bound state was obtained for soil pH value equal to 8.

Keywords:

^{137}Cs
Soil
Inventory
Vertical distribution
Convection–dispersion–fixation approach

1. Introduction

Most of the radioactive fallout coming from atmospheric nuclear weapon tests, carried out between 1955 and 1974 in South Atlantic and Pacific, have been spread in the Southern Hemisphere environmental matrices (UNSCEAR, 2000, 2008). At present, ^{137}Cs is the only anthropogenic gamma emitter found in these soils (UNSCEAR, 2000, 2008) encouraging the investigation on ^{137}Cs inventory and its transport behavior. The principal factors affecting ^{137}Cs migration in the soil are, among others, pH, organic matter content, textural class, mineralogy, competitive ions and concentration of radionuclides in the soil–liquid phase (Sawhney, 1964; Cornell, 1993; Staunton et al., 2002; Giannakopoulou et al., 2007; Singh et al., 2009). Cesium migration in soils is a very slow process and its retention is generally admitted to be controlled by weathered mica (Delvaux et al., 2000). Some micaceous minerals, such as illite and vermiculite, tend to catch Cs in their interlayers. There are two different processes to be considered, the structural fixation and the reversible selective sorption (Sawhney, 1972; Wauters et al., 1996; Poinssot et al., 1999; Konoplev et al., 2002). A fraction of ^{137}Cs might be either taken by plant roots and pasture, or reached the groundwater.

Two approaches for modeling the migration of radionuclides in soils have been used, the convection–dispersion equation (ODCDE) with constant parameters, known as the Fokker–Planck equation (Likar et al., 2001; Bossew and Kirchner, 2004) and the serial compartmental model (Kirchner, 1998; Schuller et al., 1997). The ODCDE approach is the most used model to estimate the ^{137}Cs transport parameters. However, several mechanisms such as bio-turbation and horizontal transport may induce deviations from their predictions. Moreover, irreversible retention of the ^{137}Cs by specific minerals should also be considered, particularly when their concentration in the soil is important. Some authors have developed diffusion–convection–fixation models (ODCDFE) to analyze ^{137}Cs in soil coming from the Chernobyl accident. However, the convection process was disregarded because of the short time since the accident (Antonopoulos-Domis et al., 1995; Toso and Velasco, 2001).

In Argentina, the ^{137}Cs deposit has been established in Buenos Aires city from 1960 to 2002 (Ciallella et al., 2003). Furthermore, ^{137}Cs soil profiles have been determined in the Pampa Ondulada region of Buenos Aires Province, Argentina (Bujan et al., 2000, 2003) and in natural and semi-natural grassland areas of San Luis Province (Juri Ayub et al., 2007, 2008).

Buenos Aires Province is an important agricultural and industrial area where nuclear power plants (Nucleoeléctrica Argentina, 2012) and research reactors are located (CNEA, 2012). These facilities add to

the natural inventory small amounts of anthropogenic radionuclides. Despite the long period of nuclear activity in the region and the retaken of the nuclear program in Argentina (CNEA, 2012; Carlos Rey, 2007), no systematic study has been carried out until now to establish the radiological conditions.

This article presents the determination and analysis of the ^{137}Cs inventories as well as a study of the vertical migration processes in soils of La Plata region, Buenos Aires, Argentina. A soil physico-chemical characterization was done considering the principal factors affecting the ^{137}Cs transport process. The profiles have been analyzed using the ODCFE approach (Antonopoulos-Domis et al., 1995; Toso and Velasco, 2001). To our knowledge, this is the first time that this model will be applied in a complete form, i.e., considering that the three processes, diffusion, convection and fixation simultaneously.

2. Methodology

2.1. Studied region

In the vicinity of La Plata city, two main geo-morphological units can be identified: i) the area of estuary-marine influence and ii) the area of continental influence, called hereafter coastal and inland soils, respectively. Regarding the topography, the first one is a low plain with a coast relief between 0 and 5 m above the sea level, covered by marine and fluvial deposits. Previous studies reported clay fraction from 57 to 70% in surface (Giménez et al., 2005; Hurtado et al., 2006a,b). The inland area is a high plain belonging to Pampa Ondulada, with soft undulations influenced by the loess deposits. In this area, the height above sea level is higher than 5 m in the main NW–SE watershed with a maximum altitude of 30 m. These soils presented clay contents from 26 to 35% on the topsoil (Giménez et al., 2005; Hurtado et al., 2006a,b). The average annual precipitation rate for La Plata region is 1040 mm.

2.2. Sampling

Undisturbed soils were selected in the suburb of La Plata city, Province of Buenos Aires, from the two mentioned areas: (i) SP1 and SP2 belonging to the inland area ($34^{\circ}54'27.12''\text{S}$, $58^{\circ}8'21.90''\text{W}$ and $35^{\circ}3'15.66''\text{S}$, $57^{\circ}51'12.84''\text{W}$, respectively) and (ii) SP3 and SP4 belonging to the coastal area ($34^{\circ}54'8.58''\text{S}$, $57^{\circ}55'6.00''\text{W}$ and $34^{\circ}48'27.60''\text{S}$, $58^{\circ}5'14.88''\text{W}$, respectively). The soil locations are depicted in Fig. 1. In order to assure that soils have been undisturbed at least in the last 60 years, samples were taken from natural reserves where neither sowing nor livestock have been done, and from particular farms whose owners guarantee the lack of disturbance of the selected soils. Sampling was performed down to 50 cm from the surface, taking samples at approximately 3 cm depth intervals with a $20\text{ cm} \times 20\text{ cm} \times 3\text{ cm}$ shovel. In the cases in which it was possible, 2 or 3 samples were taken to check the representativeness of the results. The samples were collected in 2009 except SP1, which was taken in 2008.

2.3. Experimental techniques

The soils pH determinations were carried out in a suspension of a 1:5 soil:distilled water (v/v) mixture (United Nations Economic Commission for Europe Convention on long-range Transboundary Air Pollution, 2006), whereas the organic carbon percentage (% OC) was established using Walkley–Black method (Claver, 1971). Soil texture was determined with an analysis of particle size by the pipette method after soil dispersion with oxygenated water and calgon (Claver, 1971).

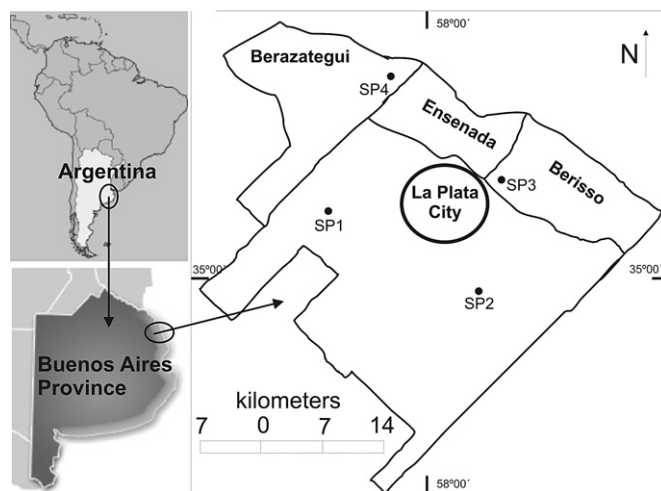


Fig. 1. Sampled sites location.

The X-ray mineralogical study was undertaken in the clay fraction. Diffractograms were obtained after saturation with magnesium and glycerol and heating to 823 K as suggested by Claver (1971). All diffraction patterns were recorded using a PANalytical, X'Pert PRO high resolution diffractometer, in the Bragg–Brentano geometry with $\text{CuK}\alpha$ radiation. The step mode collection was 0.02° , 0.02 s by step, with 2θ ranging from 3° to 32° . The mineral identification was made according to Claver (1971) and for semi-quantitative analysis, the diffraction pattern of oriented clay aggregates treated with glycol were analyzed using the PowderCell program (Kraus and Nolze, 1999). The structural data were taken from Downs and Hall-Wallace (2003). The analysis was done considering only the phyllosilicate structures.

For gamma spectroscopy, bulk samples were dried at 363 K during 48 h, crushed and sieved through a 2 mm mesh without previous separation. Before analysis, water quantity was checked using a Shimadzu TGA-50 Thermogravimeter with a heating rate of 5 K/min up to 473 K in N_2 atmosphere, being the remainder water content lower than 2 wt.%. Soil samples were placed into 2 L Marinelli-type box. The spectra were taken inside an EG&G Ortec low-background chamber in the range of 100 keV to 1.5 MeV, using a GMX10 gamma EG&G Ortec detector with a standard electronic chain and a multichannel of 8192 channels. Energy calibration was performed with ^{60}Co , ^{133}Ba , ^{137}Cs and ^{152}Eu sources and efficiency calibration was carried out using sources with the same geometry and density as the soil samples, with an admixture of known amounts of naturally occurring ^{176}Lu (99.9% purity) and ^{138}La (99.99% purity) radionuclides (Perillo Isaac et al., 1997). The soil gamma attenuation coefficients were determined (Demir et al., 2008; Montes et al., 2009) to ensure that auto-absorption effects were similar for all samples. The laboratory background was obtained and corrections in the peaks were performed. All the spectra were recorded during four days, analyzed with a commercial program. The activity concentration of ^{137}Cs was determined using the well-known 661.62 keV line. The detection limit (L_D) was 0.02 Bq/kg. Clay samples were also analyzed. In this case, spectra were taken during seven days and a clay efficiency sample was used.

2.4. Profile analyses

The ODCFE approach (Antonopoulos-Domis et al., 1995; Toso and Velasco, 2001) assumes that ^{137}Cs concentration $c(x,t)$ is composed by two fractions, a free one, $f(x,t)$, and a fixed one, $b(x,t)$ as it can be seen in equation (1):

$$c(x, t) = f(x, t) + b(x, t) \quad (1)$$

where the free state concentration is the sum of two contributions (see equation (2)):

$$\begin{cases} f(x, t) = J_0 e^{-(\lambda + k_{\text{eff}})t} \left[\frac{1}{\sqrt{\pi D_{\text{eff}} t}} e^{-\frac{(x - v_{\text{eff}} t)^2}{4 D_{\text{eff}} t}} - \frac{v_{\text{eff}}}{2 D_{\text{eff}}} e^{v_{\text{eff}} x / D_{\text{eff}}} \text{erfc} \left(\frac{v_{\text{eff}}}{2} \sqrt{\frac{t}{D_{\text{eff}}}} + \frac{x}{2 \sqrt{D_{\text{eff}} t}} \right) \right] \\ b(x, t) = k_{\text{eff}} e^{-\lambda t} \int_0^t f(x, t') dt' \end{cases} \quad (7)$$

$$f(x, t) = m(x, t) + s(x, t) \quad (2)$$

with $m(x, t)$ and $s(x, t)$ representing the mobile and reversibly sorbed concentrations.

Assuming that the rate of the fixation process of cesium is proportional to the mobile fraction ($km(x, t)$), the one-dimensional transient state mass balances for free and fixed concentrations yield to the equations system 3:

$$\begin{cases} \frac{\partial f(x, t)}{\partial t} = D \frac{\partial^2 m(x, t)}{\partial x^2} - v \frac{\partial m(x, t)}{\partial x} - \lambda f(x, t) - km(x, t) \\ \frac{\partial b(x, t)}{\partial t} = km(x, t) - \lambda b(x, t) \end{cases} \quad (3)$$

where λ is the nuclear decay constant (0.023 y^{-1} for ^{137}Cs), and D (cm^2/y), v (cm/y) and k (y^{-1}) represent the diffusion coefficient in soil water, convection velocity of water in soil pores and the rate of transfer from free to bound state, respectively. Here, x is the depth below ground surface and t is the elapsed time since the deposit ($t = \text{year of sampling minus } 1965$, where 1965 corresponds to the maximum ^{137}Cs deposit year in the studied region).

Supposing that $s(x, t)$ fraction is in equilibrium with the mobile fraction, both concentrations can be related by a linear relationship as it is shown in equation (4):

$$s(x, t) = K_D \frac{\rho_B}{\varepsilon} m(x, t) \quad (4)$$

where K_D is the distribution coefficient ($\text{cm}^3 \text{ g}^{-1}$), ρ_B is the soil bulk density (g cm^{-3}) and ε is the soil porosity.

Using equations (2) and (4) and substituting in equation (3) results (equation (5)):

$$\begin{cases} \frac{\partial f(x, t)}{\partial t} = D_{\text{eff}} \frac{\partial^2 f(x, t)}{\partial x^2} - v_{\text{eff}} \frac{\partial f(x, t)}{\partial x} - \lambda f(x, t) - k_{\text{eff}} f(x, t) \\ \frac{\partial b(x, t)}{\partial t} = k_{\text{eff}} f(x, t) - \lambda b(x, t) \end{cases} \quad (5)$$

where D_{eff} is the effective diffusion coefficient, v_{eff} refers to the effective convective velocity, and k_{eff} is the effective rate constant of fixation:

$$D_{\text{eff}} = \frac{D}{\rho_B K_D + 1}; \quad v_{\text{eff}} = \frac{v}{\rho_B K_D + 1} \quad \text{and} \quad k_{\text{eff}} = \frac{k}{\rho_B K_D + 1} \quad (6)$$

The denominator of equation (6) is frequently called the retardation factor, $R = (\rho_B K_D / \varepsilon) + 1$. It quantifies the slowdown of the vertical solute transport in soil.

Considering as initial condition at $t = 0$ a pulse-like deposit with density J_0 ($\text{Bq}/\text{cm}^2 \text{ kg}$) and a semi-infinite soil, it is possible to achieve the solution for equation (5), presented in equation (7):

A nonlinear least square analysis was done in order to estimate the model parameters J_0 , k_{eff} , D_{eff} and v_{eff} . The evaluation of parameters was conducted by fitting either the ODCDE or the ODCDFE models to the profile data, minimizing the sum of squares of residuals. For this purpose, programs were developed in MatLab® environment (MathWorks, 2008). The Nelder–Mead algorithm was applied (Nelder and Mead, 1965). Finally, standard deviations associated with optimized parameters were computed from the Jacobian matrix, following a linearization methodology in nonlinear least squares fitting (Draper and Smith, 1981).

3. Results and discussion

3.1. Soil properties

The pH value and organic carbon fraction profiles for the four analyzed soils are depicted in Fig.2. For SP1 and SP3, pH is constant in depth with values of 6.5 and 8.6, respectively. For SP2 and SP4, pH value increases with depth, being approximately 9 at 50 cm deep. These values are in agreement with data previously determined for both areas (Giménez et al., 2005; Hurtado et al., 2006a,b).

No significant differences were observed between the organic carbon fraction soil profiles, with values ranging from 0.5% to 4%, decreasing with depth in agreement with previous studies carried out at soils of Buenos Aires Province (Giménez et al., 2005; Hurtado et al., 2006a,b).

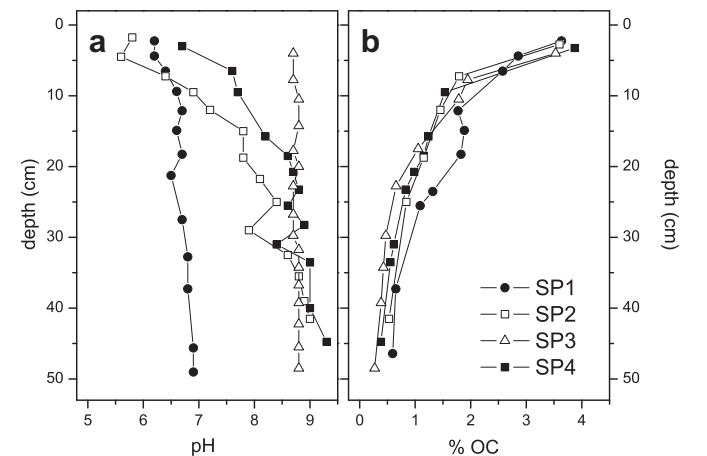


Fig. 2. a) pH and b) % OC determined profile values.

Table 1

Soil texture, textural classes and the mineralogical X-ray identification together with the relative fractions of the determined phases.

Soil	Depth (cm)	Clay (%)	Silt (%)	Sand (%)	Textural class	Illite (%)	Smectite (%)	Kaolinite (%)
SP1	2.3	26.8	67.4	5.8	Silty loam	98		2
	9.4	27.6	66.5	5.9	Silty loam/silty clay loam	99	1	
SP2	49.0	56.5	39.4	4.1	Clay	79	17	4
	1.8	15.1	64.1	20.8	Silty loam	86	10	4
	12.0	12.4	68.4	19.3	Silty loam	98		2
SP3	41.5	12.0	69.5	18.5	Silty loam	96		4
	4	35.2	54.6	10.1	Silty clay loam	48	22	30
	10.5	27.9	61.2	11.0	Silty loam/silty clay loam	50	24	27
SP4	48.5	26.0	61.3	12.8	Silty loam	37	30	32
	3.0	53.7	44.2	2.1	Silty clay	84	7	9
	15.8	70.2	27.5	2.3	Clay	64	19	17
	44.8	60.4	32.8	6.8	Clay	52	33	15

The textural classes are presented in Table 1. Significant differences were found among the studied soils; the clay fraction of coastal soils (SP3 and SP4) are higher than those of the inland soils, as reported in the literature (Giménez et al., 2005; Hurtado et al., 2006a,b).

According to X-ray diffraction patterns the identified phases are quartz, feldspar, kaolinite, illite, smectite and chlorite, respectively. The most abundant fraction corresponds to illite phyllosilicate. The results are shown in Table 1.

3.2. Inventories

The ^{137}Cs activities determined in the aforementioned soils are presented in Table 2, together with the calculated inventories. This parameter was estimated as the sum of each soil slide contribution, considering the product of the activity, the thickness and a bulk density of 1.1 g cm^{-3} (Hurtado et al., 2006a). After calculation, the resulting inventory value was reverted to 1965 the year corresponding to the maximum weapon test fallout (UNSCEAR, 2000, 2008). The average inventory value was $891 \pm 220 \text{ Bq/m}^2$, which is close to the value determined for Buenos Aires city, 1058 Bq/m^2 (Ciallella et al., 2003) and half of the values reported for Pampa Ondulada region of Buenos Aires Province, 2424 Bq/m^2 (Bujan et al., 2000, 2003). At the same south latitudinal band ($30^\circ\text{--}40^\circ$) and in central region of Argentina, San Luis Province, the evaluated local inventory ranged from 745 Bq/m^2 to 1877 Bq/m^2 (Juri Ayub et al., 2007, 2008). All values are compatible with the expected one resulting from the fallout originated from the nuclear weapon tests

Table 2

Depth measured ^{137}Cs activity concentrations and inventories referred at 1965.

SP1			SP2			SP3			SP4		
Depth (cm)	^{137}Cs (Bq/kg)	Inventory (Bq/m ²)	Depth (cm)	^{137}Cs (Bq/kg)	Inventory (Bq/m ²)	Depth (cm)	^{137}Cs (Bq/kg)	Inventory (Bq/m ²)	Depth (cm)	^{137}Cs (Bq/kg)	Inventory (Bq/m ²)
2.3	1.4 ± 0.2	829 ± 148	1.8	1.7 ± 0.3	1184 ± 178	4.0	1.4 ± 0.2	740 ± 148	3.0	4.3 ± 0.3	1095 ± 178
4.4	1.5 ± 0.2		4.5	1.7 ± 0.3		7.8	1.6 ± 0.2		6.5	1.3 ± 0.2	
6.5	1.6 ± 0.2		7.3	1.5 ± 0.2		10.5	1.8 ± 0.3		9.5	1.1 ± 0.2	
9.4	1.8 ± 0.2		9.5	1.9 ± 0.2		14.3	1.4 ± 0.3		12.5	1.1 ± 0.2	
12.1	1.7 ± 0.2		12.0	2.4 ± 0.2		17.8	0.6 ± 0.2		15.8	0.8 ± 0.2	
14.9	1.3 ± 0.2		15.0	2.3 ± 0.2		20.0	0.3 ± 0.2		18.5	0.7 ± 0.2	
18.3	0.8 ± 0.2		18.8	1.8 ± 0.2		22.8	$<L_D$		20.8	0.5 ± 0.2	
21.3	0.3 ± 0.2		21.8	0.6 ± 0.2		26.8	$<L_D$		23.3	0.5 ± 0.2	
23.5	0.2 ± 0.2		25.0	0.3 ± 0.2		29.8	$<L_D$		28.3	0.2 ± 0.2	
25.5	$<L_D$		41.5	$<L_D$		39.3	$<L_D$		33.5	$<L_D$	
29.3	$<L_D$					48.5	$<L_D$		44.8	$<L_D$	
37.3	$<L_D$										
49.0	$<L_D$										

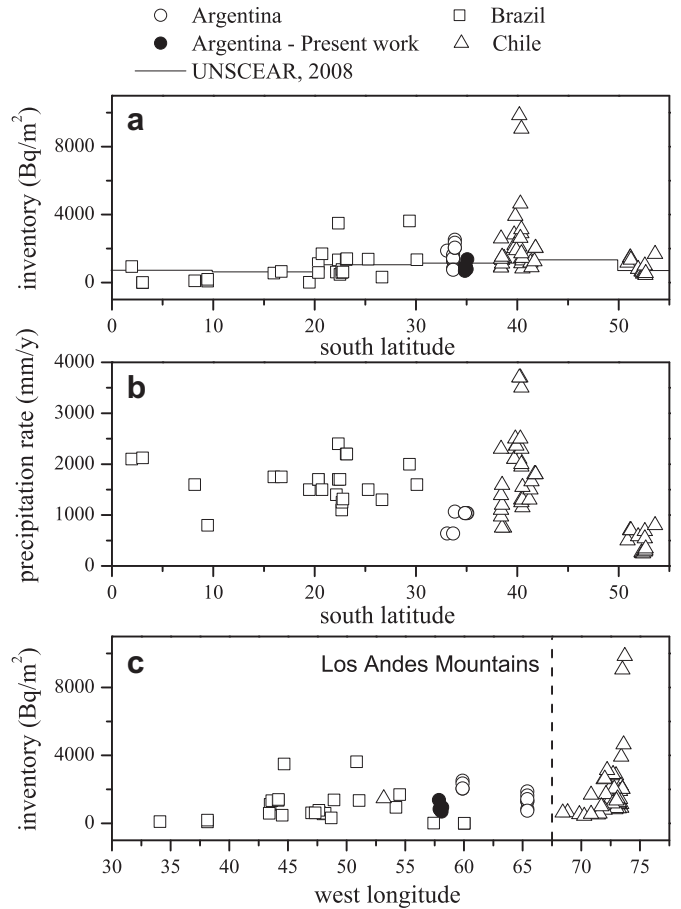


Fig. 3. a) ^{137}Cs inventories referred to 1965 vs. south latitude, b) average annual precipitation rates (solid circles) as a function of south latitude and c) inventories vs. west longitude. Data from Chile are included as open triangles (Schuller et al., 1997, 2004) and from Brazil presented as open squares (Correchel et al., 2005; Handl et al., 2008). The circles correspond to data from Argentina (solid symbols: present work, open ones: Juri Ayub et al., 2007, 2008; Bujan et al., 2000, 2003). In the figure, a) the solid line represents the UNSCEAR predictions (UNSCEAR, 2008). In the figure, c) the dashed vertical line represents the Cordillera de los Andes location.

in the Southern Hemisphere (UNSCEAR, 2000, 2008), suggesting that there was not other anthropogenic contribution in the region.

The inventories determined in La Plata region are compared in Fig. 3a to those determined in central region of Argentina (Juri Ayub et al., 2007, 2008; Bujan et al., 2000, 2003), Chile

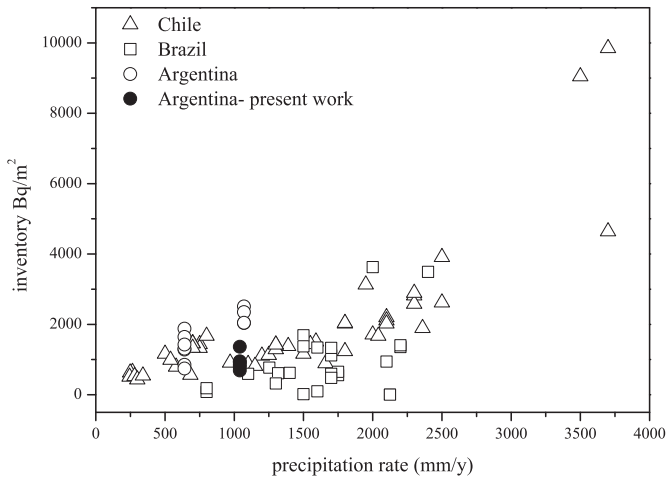


Fig. 4. ^{137}Cs inventory vs. annual precipitation rate.

(Schuller et al., 1997, 2004) and Brazil (Correchel et al., 2005; Handl et al., 2008) as a function of the latitude. In this figure the latitudinal distribution of ^{137}Cs inventories, estimated from ^{90}Sr deposition determinations assuming a $^{137}\text{Cs}/^{90}\text{Sr}$ ratio equal to 1.6 (UNSCEAR, 2000, 2008), are also included (solid line). This comparison allows us to conclude that the experimental and the predicted data match quite well, with the exception of the Chilean inventory values, reported by Schuller et al. (1997), 2004, which are systematically higher. The inventories have also been plotted in Fig. 3b as a function of the corresponding average annual precipitation rates. In Fig. 3c, the inventories vs. the west longitude are displayed together with the approximate location of the Andes Mountain. As it can be seen in Fig. 4, the ^{137}Cs inventory seems to depend on average annual precipitation. The same trend

was observed in recently published data collected in Spain (Legarda et al., 2011). In fact, a strong correlation between the average annual precipitation rate and the deposits, indistinctly of the origin (those of the Chernobyl accident and those of the weapon tests), was observed. As it can be seen in Fig. 3c, it appears that the Andes Mountain played an important role due to the generation of higher annual precipitation rates in the Chilean side of the mountains. As a result, it seems that there was more ^{137}Cs deposit on Chilean territories; it is also likely that the Andes functions as a barrier for Argentina and Brazil. This fact was corroborated after monitoring cow milk in Chile and Argentina on the same latitude, at both sides of the mountains. In this case only the milk from Chile contains trace concentrations of the anthropogenic ^{137}Cs (Desimoni et al., 2009).

3.3. Vertical migration

As it can be observed in Fig. 5, differences in the ^{137}Cs activity profiles have been detected. In general, the profiles of SP1, SP2 and SP3 seem to be typical of convective–diffusive processes (Likar et al., 2001; Bossew and Kirchner, 2004). However, SP2 profile is slightly different. It exhibits a local minimum near the surface and from 7 cm depth a convective–diffusive profile appears to be established. In the case of SP4 soil, collected at 5 km away from the La Plata river coast, the activity values are higher at the surface and decrease suddenly with a flat shape zone up to 24 cm depth. Both facts, the high values at the surface and the activity concentration profile shape, could be explained considering the fine texture (see Table 1) and the flat relief of the region, which induce water-logging. In fact, this area shows a low permeability of the underlying horizons and the phreatic water affects the deepest horizons (Imbellone et al., 2009).

Taking all these considerations in mind, SP1 and SP3 profiles were successfully fitted using the ODCDE model. Regarding SP2 sample soil, the ODCDE model did properly fit data from 7 cm deep

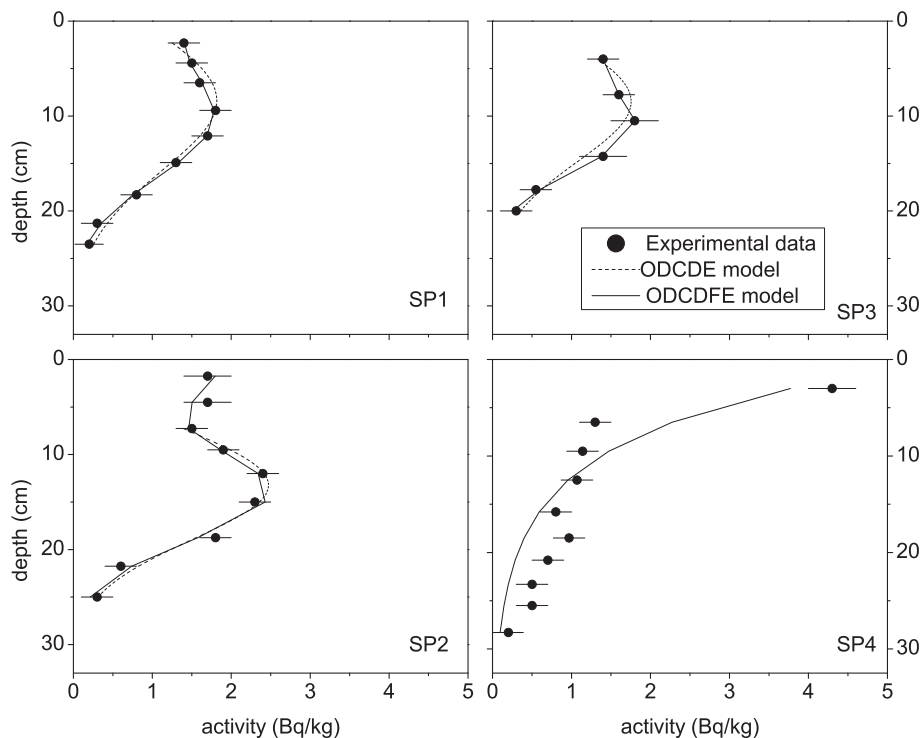


Fig. 5. ^{137}Cs activity depth concentration. Solid line and dash lines correspond to the ODCDE and ODCDFE approach fittings, respectively.

Table 3
ODCDE and ODCDFE approaches fitted parameters.

Soil	ODCDE			ODCDFE			
	J_0 (Bq cm/kg)	D_{eff} (cm ² /y)	v_{eff} (cm/y)	J_0 (Bq cm/kg)	k_{eff} (y ⁻¹)	D_{eff} (cm ² /y)	v_{eff} (cm/y)
SP1	80 ± 3	0.8 ± 0.1	0.15 ± 0.01	92 ± 4	0.011 ± 0.003	0.43 ± 0.08	0.23 ± 0.02
SP2	112 ± 13	0.8 ± 0.3	0.22 ± 0.03	138 ± 14	0.015 ± 0.003	0.33 ± 0.10	0.32 ± 0.02
SP3	69 ± 5	0.5 ± 0.1	0.16 ± 0.0	93 ± 5	0.017 ± 0.003	0.24 ± 0.05	0.25 ± 0.01
SP4				151 ± 37	0.052 ± 0.020	0.20 ^a	0.43 ± 0.20

^a Fixed value.

but efforts to reproduce the SP4 profile were fruitless. Because of the high clay fraction is mainly composed by illite, as disclosed from texture and X-ray diffraction studies, this work went a step further in the understanding of transport processes by accounting for the mechanisms of diffusion, convection and fixation process at the same time. To corroborate if ¹³⁷Cs is fixed in the clay fraction, the ¹³⁷Cs activity of this fraction was also determined. In fact, the determined activity concentrations confirmed a high retention degree with values ranging between 78 and 93% of the ¹³⁷Cs soil activity. This result supports the application of the ODCDFE model to obtain a better description of the profiles and to find reliable transport parameters.

The SP1, SP2 and SP3 ¹³⁷Cs profiles were successfully fitted by the ODCDFE model. For SP4 soil, the model fits quite well considering the observed slight discrepancies related to flood regime, which was not included in the model.

The estimated parameters including the interval of confidence for a significant level of 0.05 are reported in Table 3 and the corresponding resulting profiles are presented in Fig. 5 (solid and dashed lines correspond to ODCDFE and ODCDE, respectively). As observed in Fig. 6, D_{eff} determined using both models agrees well with South American values (Juri Ayub et al., 2007, 2008; Schuller et al., 1997, 2004) and IAEA average values (IAEA, 2010), while v_{eff} parameter values are higher than the corresponding values reported in Chile soils (Schuller et al., 1997, 2004) and the average value reported by IAEA (IAEA, 2010).

3.4. Correlations between the effective rate constant of fixation k_{eff} , the penetration depth L_p and soil properties

The profiles of organic carbon content on all the studied soils were similar; it seems that this soil property would not explain the differences in ¹³⁷Cs distributions and transport parameters.

The k_{eff} values estimated in this work were plotted in Fig. 7 as a function of average pH in the soil column where ¹³⁷Cs was detected. The maximum value is observed at pH approximately equal to 8, corresponding to SP4 soil. According to batch experiments for soils with different textural classes (Giannakopoulou et al., 2007), the maximum absorption is observed at a pH value equal to 8 approximately, in agreement with the k_{eff} maximum determined in the present study.

Another interesting parameter is the penetration depth, L_p , which is a characteristic depth for mass transport, and can be interpreted as ¹³⁷Cs average penetration depth. In the case of ODCDFE model, L_p is given by equation (8):

$$\frac{1}{L_p} = \sqrt{\left[\left(\frac{v_{\text{eff}}}{2D_{\text{eff}}} \right)^2 + \frac{k_{\text{eff}}}{D_{\text{eff}}} \right]} - \frac{v_{\text{eff}}}{2D_{\text{eff}}} \quad (8)$$

Going further in the understanding of transport processes, L_p vs. the clay content is represented in Fig. 8. There, it can be observed that penetration depth decreases with clay fraction, playing the

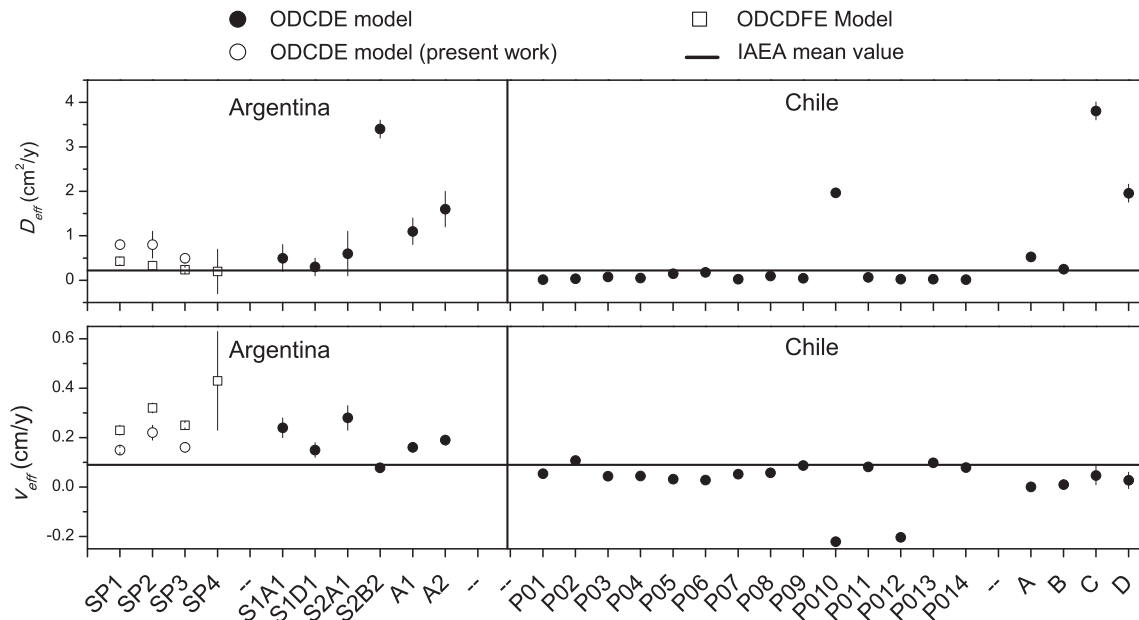


Fig. 6. Fitted D_{eff} and v_{eff} transport parameters. Open circles correspond to the present results. S1A1, S1D1, S2A1, S2B2, A1 and A2 refer to San Luis Province soils, Argentina (Juri Ayub et al., 2007, 2008), whereas P01–P014 and A, B, C and D refers to Chilean soils (Schuller et al., 1997, 2004). The vertical lines are the error bars. IAEA average values are also plotted as a dash line (IAEA, 2010).

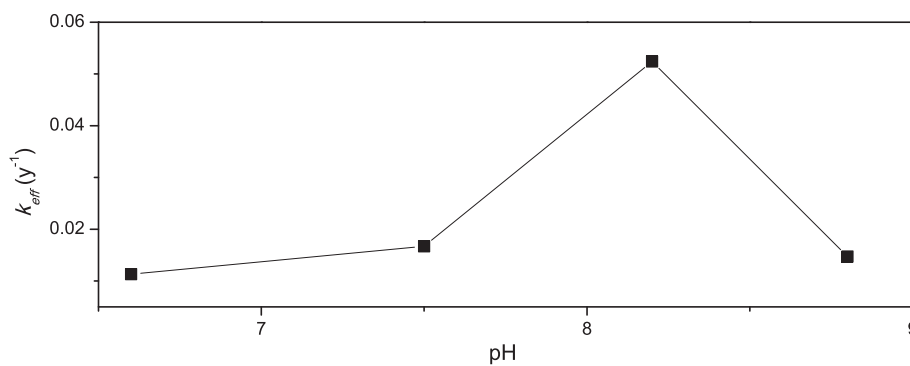


Fig. 7. Fixation rate constant k_{eff} vs. pH of the soil column.

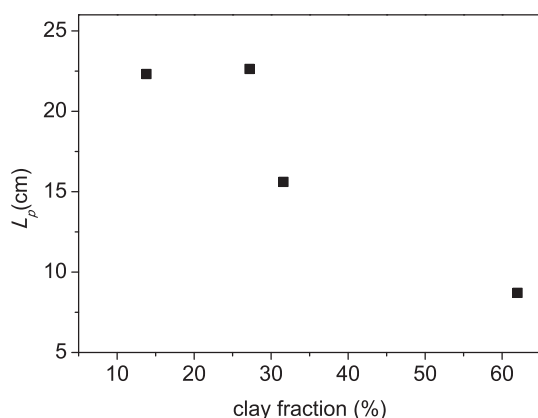


Fig. 8. Penetration depth L_p vs. clay content.

clay content a central role in depth distribution. All these experimental data did not give a definite conclusion, but it is possible to say that penetration depth depends on the clay content.

4. Conclusion

Inventories and ^{137}Cs soil profiles were determined in the vicinity of La Plata city region, Argentina. The determined inventory values are in agreement with the fallout coming from nuclear weapons atmospheric tests performed in the South Atlantic and Pacific oceans. Taking into account the information from South America, it seems that the distribution of ^{137}Cs inventory in latitudinal bands is perturbed by the presence of the Andes Mountain, which acts as a natural barrier for precipitation and wind circulation. These facts produce a high deposit on Chile region. The values seem to depend on the average annual precipitation rate more than on the latitudinal location of the sampled sites.

Concerning the activity profiles, the most used approach, the convection–dispersion with constant parameters, did not reproduce all profiles satisfactorily, probably due to the predominance of illite phase in the soils, a known receptor of cesium in an irreversibly way. In this frame, the convection–diffusion–fixation model was used, and all the profiles could be reproduced. Although the SP4 ^{137}Cs profile fit using the convection–diffusion–fixation model is not perfect, it is still a better approach than the model without fixation. However, the contribution of other processes should be considered to reach a more confident interpretation of the profile.

The effective diffusion coefficient and the effective convection velocity values were in accordance with those determined for other

regions of the Southern Hemisphere. The estimated rate constant of fixation showed a maximum for soil pH equal to 8.

Finally, it is tempting to conclude that penetration depth decreases with clay fraction, having the clay content a relevant role when referring to depth distribution. This fact is intimately related to the increase in the Cs transfer rate from mobile to bounded states as the clay content of the soil increases.

Acknowledgments

Research grants PIP 0230 from Consejo Nacional de Investigaciones Científicas y Técnicas (CONICET, Argentina) and PICT 38047-Préstamo BID from Agencia de Promoción Científica (ANCYT, Argentina) are gratefully recognized. We gratefully acknowledge to Laboratorio de difracción de rayos X y análisis térmico-diferencial-Centro de Investigaciones Geológicas-CONICET for the X-ray diffraction analysis. MLM is also indebted to Florencia Paez, who helped on reading the manuscript.

References

- Antonopoulos-Domis, M., Clouvas, A., Hiladakis, A., Kadi, S., 1995. Radiocesium distribution in undisturbed soil: measurements and diffusion-advection model. *Health Phys.* 69 (6), 949–953.
- Bossey, P., Kirchner, G., 2004. Modelling the vertical distribution of radionuclides in soil. Part 1: the convection–dispersion equation revisited. *J. Environ. Radioact.* 73, 127–150.
- Bujan, A., Santanatoglia, O.J., Chagas, C., Massobrio, M., Castiglioni, M., Yañez, M., Ciallella, H., Fernandez, J., 2000. Preliminary study on the use of the ^{137}Cs method for soil erosion investigation in the pampean region of Argentina. *Acta Geol. Hisp.* 35, 271–277.
- Bujan, A., Santanatoglia, O.J., Chagas, C., Massobrio, M., Castiglioni, M., Yañez, M., Ciallella, H., Fernandez, J., 2003. Soil erosion evaluation in a small basin through the use of ^{137}Cs technique. *Soil Till. Res.* 69, 127–137.
- Carlos Rey, D.F., 2007. Reactivación del plan nuclear Argentino. www.pagina12.com.ar.
- Ciallella, H.E., Fernandez, J.A., Lewis, E.C., Quintana, E.E., 2003. Niveles ambientales de ^{90}Sr y ^{137}Cs Provenientes del fallout en la República Argentina. VII Congreso Argentino de Protección Radiológica y Seguridad Nuclear.
- Claver, R., 1971. *Procedure in Sedimentary Petrology*. Wiley Interscience, New York.
- CNEA, 2012. <http://www.cnea.gov.ar/>.
- Cornell, R.M., 1993. Adsorption of cesium on minerals: a review. *J. Radioanal. Nucl. Chem.* 171 (2), 483–500.
- Correche, V., Oliveira Santos Bacchi, O., Reichardt, K., Cereci de Maria, I., 2005. Random and systematic spatial variability of ^{137}Cs inventories at reference sites in south-central Brazil. *Sci. Agric.* 62, 173–178.
- Delvaux, B., Kruyts, N., Cremers, A., 2000. Rhizospheric mobilization of radiocesium in soils. *Environ. Sci. Tech.* 34, 1489–1493.
- Demir, D., Un, A., Ozgul, M., Sahin, Y., 2008. Determination of photon attenuation coefficient, porosity and field capacity of soil by gamma ray transmission for 60 keV, 356 keV and 662 keV gamma rays. *Appl. Radiat. Isot.* 12, 1834–1837.
- Desimoni, J., Sives, F., Errico, L., Taylor, M.A., 2009. Activity levels of gamma-emitters in Argentinean cow milk. *J. Food Comp. Anal.* 22, 250–253.
- Downs, R.T., Hall-Wallace, M., 2003. *American Mineralogist Crystal Structure Database*. <http://ruff.geo.arizona.edu/AMS/amcsd.php>.
- Draper, N.R., Smith, H., 1981. *Applied Regression Analysis*, second ed. John Wiley & Sons, New York.

- Giannakopoulou, F., Haidouti, C., Chronopoulou, A., Gasparatos, D., 2007. Sorption behavior of cesium on various soils under different pH levels. *J. Hazard. Mater.* 149, 553–556.
- Giménez, J.E., Cabral, M.G., Hurtado, M.A., 2005. In: Comisión de Investigaciones Científicas de la Provincia de Buenos Aires (Ed.), *Elaboración y Transferencia de cartografía Temática e Implementación de un Sistema de Información Geográfica para el Planeamiento (Partido de Berisso)*. Universidad Nacional de La Plata.
- Handl, J., Sachse, R., Jakob, D., Michel, R., Evangelista, H., Goncalves, A.C., de Freitas, A.C., 2008. Accumulation of ^{137}Cs in Brazilian soils and its transfer to plants under different climatic conditions. *J. Environ. Radioact.* 99, 271–287.
- Hurtado, M.A., Giménez, J.E., Cabral, M.G., 2006a. Análisis ambiental del partido de La Plata. In: Consejo Federal de Inversiones (Ed.), *Aportes al ordenamiento territorial*. Universidad Nacional de La Plata.
- Hurtado, M.A., Giménez, J.E., Cabral, M.G., 2006b. In: *Suelos del partido de Berazategui como base para el planeamiento ambiental y ordenamiento territorial. Contrato de Obra entre Consejo Federal de Inversiones y Facultad de Ciencias Naturales y Museo*. (Ed.). Universidad Nacional de La Plata.
- IAEA, 2010. *Handbook of Parameter Values for the Prediction of Radionuclide Transfer in Terrestrial and Freshwater Environments*. Technical Report Series No. 472, Vienna.
- Imbellone, P.A., Guichon, B.A., Giménez, J.E., 2009. Hydromorphic soils of the Rio de la Plata coastal plain, Argentina. *Lat. Am. J. Sedimentol. Basin Anal.* 16, 3–18.
- Juri Ayub, J., Rizzotto, M., Toso, J., Velasco, H., 2007. ^{137}Cs deposition and vertical migration in soils from Argentina. In: *Proc. International. Conf. on Environ. Radioactivity: From Measurements and Assessments to Regulation*, Vienna, Austria. www-pub.iaea.org/mtcd/meetings/announcements.asp?confid=145.
- Juri Ayub, J., Velasco, R.H., Rizzotto, M., Quintana, E., Aguiar, J., 2008. ^{40}K , ^{137}Cs and ^{226}Ra soil and plant content in semi-natural grasslands of Central Argentina. In: Paschoa, A.S. (Ed.), *The Natural Radiation Environment—8th International Symposium*. American Institute of Physics.
- Kirchner, G., 1998. Applicability of compartmental models for simulating the transport of radionuclides in soil. *J. Environ. Radioact.* 38, 339–352.
- Konoplev, A., Kaminski, S., Klemm, E., Konopleva, I., Miller, R., Zibold, G., 2002. Comparative study of ^{137}Cs partitioning between solid and liquid phases in Lakes Constance, Lugano and Vorsee. *J. Environ. Radioact.* 58, 1–11.
- Kraus, W., Nolze, G., 1999. *Federal Institute for Mater PowderCell for Windows Version 2.3*.
- Legarda, F., Romero, L.M., Herranz, M., Barrera, M., Idoeta, R., Valiño, F., Olondo, C., Caro, A., 2011. Inventory and vertical migration of ^{137}Cs in Spanish mainland soils. *J. Environ. Radioact.* 102, 589–597.
- Likar, A., Omahem, G., Lipoglavsek, M., Vidmar, T., 2001. A theoretical description of diffusion and migration of ^{137}Cs in soil. *J. Environ. Radioact.* 57, 191–201.
- MathWorks, 2008. *Matlab, the Language of Technical Computing*. Version 7.3.0.324 (Release 2008a), Mathworks Inc..
- Montes, M.L., Taylor, M.A., Runco, J., Errico, L., Martinez, J.Y., Desimoni, J., 2009. Implementación de la técnica de espectroscopía gamma para la determinación de humedad en suelos. *ANALES AFA* 20, 205–207.
- Nelder, J.A., Mead, R., 1965. A simplex method for function minimization. *Comput. J.* 7 (4), 308–313.
- Nucleoeléctrica Argentina, 2012. <http://www.na-sa.com.ar>.
- Perillo Isaac, M.C., Hurley, D., McDonald, R.J., Norman, E.B., Smith, A.R., 1997. A natural calibration source for determining germanium detector efficiencies. *Nucl. Instr. Meth. Phys. Res. A* 397, 310–316.
- Poinssot, C., Baeyens, B., Bradbury, M.H., 1999. Experimental and modelling studies of caesium sorption on illite. *Geochim. Cosmochim. Acta* 63, 3217–3227.
- Sawhney, B.L., 1964. Sorption and fixation of microquantities of cesium by clay minerals: effect of saturating cations. *Soil Sci. Soc. Am. Proc.* 28, 183–186.
- Sawhney, B.L., 1972. Selective sorption and fixation of cations by clays minerals: a review. *Clays Clay Miner* 20, 93–100.
- Schuller, P., Ellies, A., Kirchner, G., 1997. Vertical migration of fallout ^{137}Cs in agricultural soils from southern Chile. *Sci. Total Environ.* 193, 197–205.
- Schuller, P., Bunzl, K., Voigt, G., Ellies, A., Castillo, A., 2004. Global fallout ^{137}Cs accumulation and vertical migration in selected soils from South Patagonia. *J. Environ. Radioact.* 71, 43–60.
- Singh, B.K., Jain, A., Kumar, S., Tomar, B.S., Tomar, R., 2009. Role of magnetite and humic acid in radionuclide migration in the environment. *J. Contam. Hydrol.* 106, 144–149.
- Staunton, S., Dumat, C., Zsolnay, A., 2002. Possible role of organic matter in radio-caesium adsorption in soils. *J. Environ. Radioact.* 58, 163–173.
- Toso, J.P., Velasco, R.H., 2001. Describing the observed vertical transport of radio-caesium in specific soils with three time-dependent models. *J. Environ. Radioact.* 53, 133–144.
- United Nations Economic Commission for Europe Convention on long-range Transboundary Air Pollution, 2006. *Soil Anal. Meth. 6 (SA06)*. Manual on Methods and Criteria for Harmonized Sampling, Assessment, Monitoring and Analysis of the Effects of Air Pollution on Forests.
- UNSCEAR, 2000. *Sources and Effects of Ionizing Radiation*. Report of the General Assembly with Scientific Annexes, New York.
- UNSCEAR, 2008. *Sources and Effects of Ionizing Radiation*. Report of the General Assembly with Scientific Annexes, New York.
- Wauters, J., Elsen, A., Cremers, A., 1996. Prediction of solid/liquid distribution coefficients of radio-caesium in soils and sediments. Part one: a simplified procedure for the solid phase characterization. *Appl. Geochem.* 11, 589–594.